Available online at www.sciencedirect.com

ScienceDirect

Advances in Climate Change Research 12 (2021) 871−880

www.keaipublishing.com/en/journals/accr/

Modelling the effect of local and regional emissions on $PM_{2.5}$ concentrations in Wuhan, China during the COVID-19 lockdown

BAI Yong-Qing[a], WANG Ying[b], KONG Shao-Fei[c], ZHAO Tian-Liang[b,*], ZHI Xie-Fei[b], ZHENG Huang[c], SUN Xiao-Yun[b], HU Wei-Yang[b], ZHOU Yue[a], XIONG Jie[a]

[a] *Hubei Key Laboratory for Heavy Rain Monitoring and Warning Research, Institute of Heavy Rain, China Meteorological Administration, Wuhan, 430205, China*
[b] *Key Laboratory of Meteorological Disaster, Ministry of Education & Collaborative Innovation Center on Forecast and Evaluation of Meteorological Disasters, Key Laboratory for Aerosol-Cloud-Precipitation of China Meteorological Administration, Nanjing University of Information Science and Technology, Nanjing, 210044, China*
[c] *Department of Atmospheric Sciences, School of Environmental Studies, China University of Geosciences, Wuhan, 430074, China*

Received 14 February 2021; revised 22 September 2021; accepted 26 September 2021
Available online 19 October 2021

Abstract

$PM_{2.5}$ concentrations in Wuhan, China decreased by 36.0% between the period prior to the COVID-19 pandemic (1−23 January, 2020) and the COVID-lockdown period (24 January to 29 February, 2020). However, decreases in $PM_{2.5}$ concentration due to regional $PM_{2.5}$ transport driven by meteorological changes, and the relationship between the $PM_{2.5}$ source and receptor, are poorly understood. Therefore, this study assessed how changes in meteorology, local emissions, and regional transport from external source emissions contributed to the decrease in Wuhan's $PM_{2.5}$ concentration, using FLEXPART-WRF and WRF-Chem modelling experiments. The results showed that meteorological changes in central China explain up to 22.2% of the total decrease in $PM_{2.5}$ concentrations in Wuhan, while the remaining 77.8% was due to air pollutant emissions reduction. Reduction in air pollutant emissions depended on both local and external sources, which contributed alomst equally to the reduction in $PM_{2.5}$ concentrations (38.7% and 39.1% of the total reduction, respectively). The key emissions source areas affecting $PM_{2.5}$ in Wuhan during the COVID-lockdown were identified by the FLEXPART-WRF modeling, revealing that regional-joint control measures in key areas accounted for 89.3% of the decrease in $PM_{2.5}$ concentrations in Wuhan. The results show that regional-joint control can be enhanced by identifying key areas of emissions reduction from the source−receptor relationship of regional $PM_{2.5}$ transport driven by meteorology under the background of East Asian monsoon climate change.

Keywords: COVID-19; $PM_{2.5}$; Regional transport; Emissions reduction; Regional-joint control

1. Introduction

The outbreak and spread of the coronavirus disease (COVID-19) caused an unprecedented disruption in social activities and the environment (Shi and Brasseur, 2020; Tian et al., 2020; Hammer et al., 2021; Zheng et al., 2021). Worldwide lockdowns have decreased air pollution and greenhouse gas emissions due to reduced transportation, electricity generation, and industrial production (El-Sayed et al., 2021; Zangari et al., 2020; Kumar and Dwivedi, 2021; Yang et al., 2021). It is important to explore how the social changes resulted from the COVID-19 lockdown contribute to low-carbon pathways (Rosenbloom and Markard, 2021).

Significant reductions in air pollutant concentrations have been seen in many regions of the world, indicating that isolation measures had a positive effect on short-term improvements in air quality (Dai et al., 2020; Mahato et al.,

* Corresponding author.
E-mail address: tlzhao@nuist.edu.cn (ZHAO T.-L.).
Peer review under responsibility of National Climate Center (China Meteorological Administration).

https://doi.org/10.1016/j.accre.2021.09.013

2020; Shi and Brasseur, 2020; Munir et al., 2021; Vega et al., 2021). Satellite measurements have shown a 48% drop in tropospheric NO_2 vertical column densities over China (Liu et al., 2020a), and in New York city concentrations of $PM_{2.5}$ and NO_2 have decreased by 36% and 51%, respectively (Zangari et al., 2020). Several studies have also investigated the impact of the COVID-19 pandemic on the environment and climate change (Forster et al., 2020; Grewe et al., 2021). The reduced anthropogenic emissions caused by the COVID-19 restrictions had a positive effect on the hydrological cycle over South Asia (Fadnavis et al., 2021), and reduced the quantity of short-lived climate pollutants at remote locations above atmospheric boundary layer over northern Italy (Paolo et al., 2021). Rosenbloom and Markard (2021) have also argued the importance of leveraging COVID-19 recovery to advance the transition to a low-carbon society.

China's lockdown measures led to a significant reduction in pollution emissions and pollutant concentrations (Bao and Zhang, 2020; Chen et al., 2020; Fan et al., 2020; Liu et al., 2020b; Pei et al., 2020). However, the benefits of emissions reduction was reduced by adverse meteorology, and severe air pollution events still occurred in China during the COVID-19 lockdowns (Wang et al., 2020). The unexpected heavy haze that occurred in northern China was mainly due to the enhancement of secondary pollution through heterogeneous reactions under high ambient relative humidity, in conjunction with stagnant air conditions (Le et al., 2020; Huang et al., 2020; Sun et al., 2020). Cross-regional transport of air pollutants from the upstream zone in turn led to haze pollution in the downstream zone. For example, during long-range transport events regional scale air pollutants likely contributed 40%−90% of the $PM_{2.5}$ concentration in the Hangzhou urban area (Yuan et al., 2020). Particulate nitrate formation in Shanghai was facilitated and enhanced by long-range and regional transport (Chang et al., 2020). The long-range transport of air pollutants also substantially contributed to $PM_{2.5}$ pollution in Hubei, reflecting the importance of meteorological conditions in regional air quality (Shen et al., 2020). Therefore, air pollution prevention and control should not only focus on local pollution emissions sources, but also on the impact of cross-regional transport of air pollutants. This highlights the importance of regional-joint control in pollution management (Griffith et al., 2020; Li et al., 2020; Zheng et al., 2020).

In recent years, there has been significant attention around the impact of both meteorological conditions and emissions control measures on changes in $PM_{2.5}$ concentration, using air quality modelling (Xu et al., 2018; Cheng et al., 2019; Zhou et al., 2019; Zhang et al., 2020). The Weather Research and Forecasting model coupled with Chemistry (WRF-Chem) implements the two-way coupling of atmospheric dynamics and atmospheric chemistry. It includes chemical processes such as pollutant transport, wet and dry deposition, gas-phase chemistry, aerosol formation, radiation and photolysis rates, and aerosol parameterisation for chemical models online, and is widely used in atmospheric environmental research (Grell et al., 2005; Kumar et al., 2014; Zhong et al., 2016; Lennartson et al., 2018; Zhou et al., 2019). Jiang et al. (2021) applied the WRF-Chem model in combination with surface observations in southern California, and found that emissions reduction was responsible for 68% of the decrease in $PM_{2.5}$ concentration before and after the lockdown, while meteorology variations where responsible for the remaining 32%. Yin et al. (2021) found that in Hubei province, which saw most of China's pneumonia cases, emissions reduction was responsible for a reduction in $PM_{2.5}$ concentrations by 72% in February 2020, which exceeded the 13% increase caused by meteorology. The short-term impact of lockdown on air quality in Wuhan has been reported: $PM_{2.5}$ concentrations decreased by 36.9% during lockdown relatively to the pre-lockdown period (Lian et al., 2020; Shi and Brasseur, 2020); it was predominantly contributed by the emission reduction (92.0%) compared with the same period in 2019, by retrieving from a random forest tree approach (Zheng et al., 2020). However, the contributions of meteorology, local emissions, and regional transport from external source emissions to the decrease in $PM_{2.5}$ concentration have not yet been quantitatively assessed in detail.

Hubei province, which borders the North China Plain in the north and the Yangtze River Delta region in the east, features a distinct regional transport of air pollution. Previous studies have shown that in winter, the prevailing northerly winds drive the cross-regional transport of air pollutants from North China and the Yangtze River Delta region, which significantly increases haze pollution in Wuhan (Yue et al., 2016; Lu et al., 2017; Li et al., 2019; Zheng et al., 2019; Yu et al., 2020). Regional-joint control of air pollution across administrative boundaries is therefore necessary to improve regional air quality (Zhang et al., 2016; Chang et al., 2019). However, the management mechanisms of regional-joint control at the provincial level between Hubei and its surrounding provinces have not yet been established.

Chinese government imposed a lockdown in Wuhan on 23 January 2020, and extended the lockdown to the whole province, and even nationwide, several days later, in an attempt to quarantine the epicentre of the COVID-19 outbreak (Le et al., 2020). The cessation of human activities during the COVID-19 lockdown can be considered as a passive regional-joint control of air pollution. Existing emissions reduction measures during important activities or heavy pollution periods are mostly designed for temporary regions or short-term time scales. However, the spatial and temporal scales of these measures are significantly smaller than the scale of the COVID-19 lockdowns. The response of $PM_{2.5}$ concentration during extreme emissions reduction scenarios deserves further research. In this study, the effect of meteorological changes, local emissions reduction, and passive regional-joint control on the decrease in $PM_{2.5}$ concentration in Wuhan, was assessed based on WRF-Chem emissions reduction scenarios for COVID-19 lockdowns. The aim was to improve our understanding of the causes of local air quality changes during the COVID-19 pandemic.

2. Data and methods

2.1. Observational data

Hourly observations of meteorological data, including 2-m air temperature, 2-m relative humidity, and 10-m wind speed, in Wuhan from 1 January to 29 February 2020, and in the same period in 2019, were obtained from the Hubei Meteorological Service (http://data.cma.cn/). Hourly $PM_{2.5}$ concentrations in Wuhan for the same time periods were obtained from the Department of Ecology and Environment of Hubei Province (http://sthjt.hubei.gov.cn/hjsj/sjfb/). In addition, hourly observations of the chemical compositions of $PM_{2.5}$, including water-soluble ions (SO_4^{2-}, NO_3^-, and NH_4^+), trace elements (TE), organic carbon (OC), and elemental carbon (EC), were conducted using online instruments from 1 January to 29 February 2020, at an environmental monitoring supersite in Wuhan. All instruments were actively maintained and regularly calibrated by detailed quality assurance and quality control, and the relative standard deviation was limited to within 10% (Zheng et al., 2020).

We divided the study period into two phases, pre-COVID (1−23 January 2020) and COVID-lock (24 January−29 February 2020).

2.2. Adjustment of the base emissions during the pre-COVID phase

We used the Multi-resolution Emission Inventory for China (MEIC) (http://www.meicmodel.org/) for 2016 to obtain the base anthropogenic emissions. The inventory provided data on anthropogenic pollutants and greenhouse gas emissions for ten major atmospheric chemical constituents, including SO_2, NO_x, CO, NH_3, NMVOC, $PM_{2.5}$, BC, and OC. The monthly gridded emissions data are at $0.25^\circ \times 0.25^\circ$ spatial resolution for five emissions sectors, including power, industry, transport, residential, and agriculture, meeting the simulation requirements of multi-scale atmospheric chemistry models (Li et al., 2017).

Owing to the lack of detailed emissions data, which often take years to update, the emissions level in the most recent period was projected using the year-by-year reduction ratio of MEIC inventory emissions by Zheng et al. (2018). We scaled the 2013 emissions to the 2020 levels according to the relative changes for 2013−2017 in China from the MEIC trend report (Zheng et al., 2018), assuming that emissions in 2018−2020 followed the same trend. We calculated the anthropogenic emissions of eight species in 2020 using quadratic function fitting based on the total emissions during 2013−2017 (Jiang et al., 2021). With the 2016 MEIC inventory and reduction ratios of 2020 relative to 2016, the WRF-Chem model was used to simulate the $PM_{2.5}$ concentration in Wuhan in the pre-COVID phase. Based on the simulation results, we adjusted the emissions intensity by several iterations of abatement (Xue et al., 2021), until the simulation results were reasonable and the absolute value of the normalised mean bias (NMB) of the simulation results and observations was less than 10%.

2.3. Identifying $PM_{2.5}$ footprints using FLEXPART-WRF

The regional transport of source−receptor air pollutants is typically complicated by emissions and meteorological factors. The FLEXPART-WRF Lagrange particle model was used to identify the distribution of potential source regions (footprints) that may have had an impact on the receptor site. Wuhan was set as the pollutant receptor site, and a large number of $PM_{2.5}$ tracer particles were released hourly every day, using backward integration for 48 h. Thus, the residence time (s) of the released particles on the near-ground grid was simulated. By multiplying the residence time by the $PM_{2.5}$ emission intensity ($\mu g\ m^{-2}\ s^{-1}$) on the corresponding grid, the $PM_{2.5}$ footprints in Wuhan ($\mu g\ m^{-2}$) were calculated. The potential contribution of extra-provincial sources to $PM_{2.5}$ concentration in Wuhan was estimated from the proportion of extra-provincial footprints to the total regional footprints.

2.4. Experimental design and analysis method

The COVID-19 lockdown provided an unexpected experiment of air pollutant emissions control in China. A series of WRF-Chem experiments with different emissions reduction scenarios were designed to simulate $PM_{2.5}$ concentrations in Wuhan during the pre-COVID and COVID-lock phases. These experiments were designed to evaluate how meteorological changes and regional emissions reduction in China impacted the decrease in $PM_{2.5}$ concentration, and to determine how emissions reduction in Hubei and its surrounding areas contributed to the decrease in $PM_{2.5}$ concentration. More detailed information can be found in Tables 1 and 2.

Table 1
Design of WRF-Chem sensitivity experiments.

Experiment	Emissions reduction scenario	Meteorological simulation phase	Mean of simulated (observed) $PM_{2.5}$ concentration in Wuhan ($\mu g\ m^{-3}$)
C1pre	Adjusted pre-COVID emissions	Pre-COVID	58.9 (63.3)
C2pre	30% regional emissions reduction in China	Pre-COVID	42.4
C1	Adjusted pre-COVID emissions	COVID-lock	54.2
C2	30% regional emissions reduction in China	COVID-lock	39.3 (40.5)
C3	30% emissions reduction in Hubei	COVID-lock	46.8
C4	30% emissions reduction in Hubei and its surrounding areas	COVID-lock	40.9
C5	50% emissions reduction in Hubei	COVID-lock	40.7
C6	50% emissions reduction in the Wuhan City circle	COVID-lock	41.7

Table 2
Experimental analysis methods and description during the pre-COVID and COVID-lock phases (relative to the decrease in $PM_{2.5}$ concentration in Wuhan).

Period	Method	Description
From the pre-COVID to COVID-lock	(C1 − C1pre)/C1pre	Impact of meteorological changes
	(C2pre − C1pre)/C1pre	Impact of regional emissions reduction in China
	(C2 − C1pre)/C1pre	Impact of meteorological changes and regional emissions reduction in China
	(C1 − C1pre)/(C1 − C1pre + C2pre − C1pre)	Contribution of meteorological changes
	(C2pre − C1pre)/(C1 − C1pre + C2pre − C1pre)	Contribution of regional emissions reduction in China
COVID-lock	(C2 − C1)/C1	Impact of regional emissions reduction in China
	(C3 − C1)/C1	Impact of emissions reduction in Hubei
	(C4 − C3)/C1	Impact of emissions reduction in the surrounding areas
	(C2 − C4)/C1	Impact of emissions reduction in other regions
	(C3 − C1)/(C2 − C1)	Contribution of emissions reduction in Hubei
	(C4 − C3)/(C2 − C1)	Contribution of emissions reduction in the surrounding areas
	(C2 − C4)/(C2 − C1)	Contribution of emissions reduction in other regions

The simulation of the Wuhan $PM_{2.5}$ concentration showed a substantial reduction, with the main pollutants decreasing by approximately 30% in February 2020 (Zheng et al., 2021). This was in agreement with the observed emissions reduction of 30% (Table 1, C2 experiment).

According to the pathways of atmospheric circulation-driven regional $PM_{2.5}$ transport (see Section 3.3) and wind rose for Wuhan during the COVID-lock phase (Fig. 1a), the key areas surrounding Hubei (Henan, Shandong, Anhui, Jiangsu, and Jiangxi provinces) (Fig. 1b, Table 1) were identified as areas of regional-joint control. Other areas outside of Hubei and the surrounding areas are referred to as other regions (Table 2). The emissions reduction refers to the decreasing degree of anthropogenic emissions during the COVID-lock phase compared to the pre-COVID phase, including all sectors and all species of air pollutants in the inventory.

2.5. WRF-chem configuration and evaluation

We utilised WRF-Chem to quantify the roles of emissions and meteorological conditions in the changes in $PM_{2.5}$ concentration during the COVID-19 pandemic. The Regional Environmental Meteorological Numerical Forecast System in Central China, with the WRF-Chem model as the core, has made accurate forecasts in previous operational evaluations and applications (Liu et al., 2018; Bai et al., 2016, 2020). A two-nested domain was set for the simulations, based on the framework of the model. The outer domain covered most of East Asia, and consisted of 370 × 214 grids with a grid spacing of 27 km. The inner domain covered Central China and had 250 × 190 points with a grid spacing of 9 km. The vertical 34 hybrid layers were set from the surface to 50 hPa. The main physicochemical parameterisation schemes included the YSU boundary layer scheme, RRTM longwave radiation scheme, Goddard shortwave radiation scheme, Noah LSM land surface model, RADM2 gas phase chemistry, and MADE/SORGAM aerosol chemistry mechanism.

WRF-Chem was used to design multiple emissions scenario experiments to simulate changes in $PM_{2.5}$ concentration from 1 January to 29 February 2020, using a 1° × 1° resolution. Final Operational Global Analysis (FNL) was used as the atmospheric initial and boundary conditions, and the side boundary was updated every 6 h and integrated continuously during the study period. The nudging four-dimensional

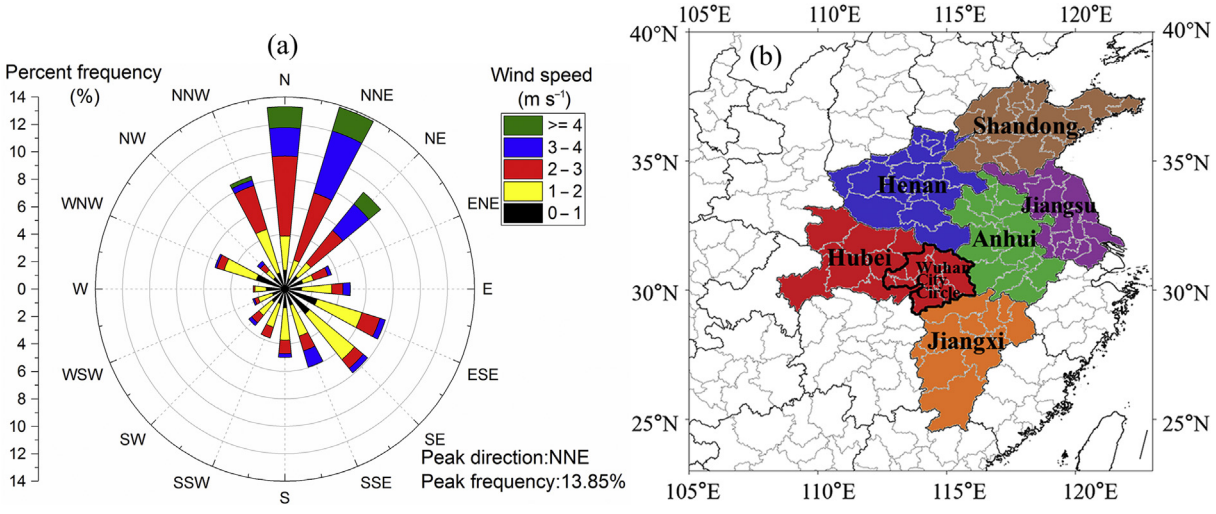

Fig. 1. (a) Wind rose for Wuhan during the COVID-lock phase and (b) the administrative map of Hubei province and its surrounding areas (Henan, Shandong, Anhui, Jiangsu, and Jiangxi provinces). The Wuhan city circle in Hubei is outlined with thick black lines.

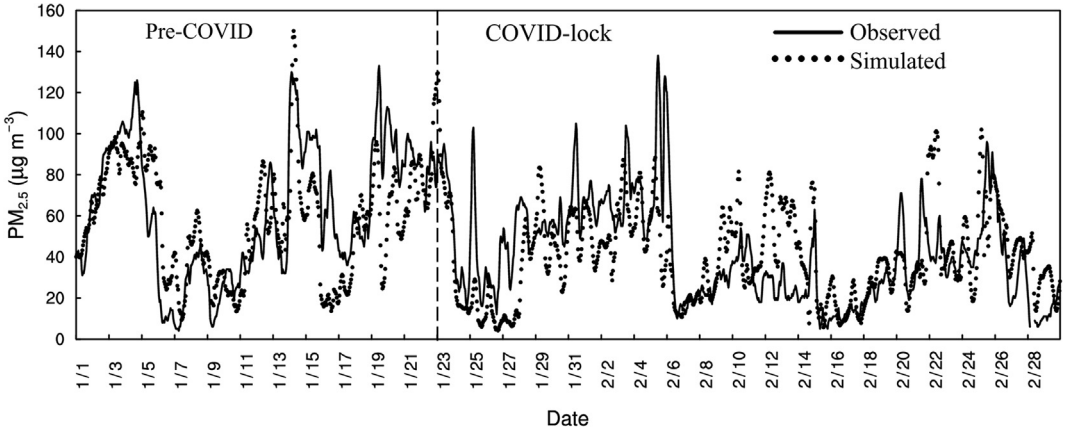

Fig. 2. Observed and simulated hourly $PM_{2.5}$ concentration in Wuhan from 1 January to 29 February 2020 (The vertical dashed line indicates the start of the lockdown in Wuhan. The C1pre experiment was used for the pre-COVID phase, and the C2 experiment was used for the COVID-lock phase).

assimilation process was applied to relax the model output to observation, and the 0−72 h model spin-up time was excluded from each experiment. The high spatial resolution MEIC (0.25° × 0.25°) in 2016 was applied as the basic anthropogenic emissions.

The influence of temperature, humidity, and wind on $PM_{2.5}$ concentrations across China was much larger than that of other meteorological factors (Chen et al., 2018). Hourly meteorological observation data and urban air quality data in Wuhan from 1 January to 29 February 2020 were used to examine the simulation of ambient temperature, humidity, wind speed, and $PM_{2.5}$ concentration in the Wuhan area during the COVID-lock using the WRF-Chem model. The examination showed that WRF-Chem performed well in simulating meteorological parameters before and during the lockdown (most correlation coefficients were higher than 0.7; Table A1), with slightly low humidity and slightly high temperature and wind speed.

Fig. 2 shows the observed and simulated hourly $PM_{2.5}$ concentrations in Wuhan from 1 January to 29 February 2020 where C1pre and C2 are based on the adjusted emissions in the pre-COVID and COVID-lock phases, respectively. The simulation results represent the 'actual' changes in $PM_{2.5}$ concentration (Fig. 2). WRF-Chem accurately simulated the $PM_{2.5}$ pollution process, peak concentrations, and evolution during the pre-COVID and the lockdown phases. The simulated mean $PM_{2.5}$ values were close to the observed values during both phases (Table 1), with correlation coefficients of 0.7 and 0.5, respectively (Table A1). The observed $PM_{2.5}$ concentration decreased by 22.8 μg m^{-3} (36.0%) during the COVID-lock phase relative to pre-COVID, while the simulated $PM_{2.5}$ concentration decreased by 19.6 μg m^{-3} (33.3%). This further validates the reasonableness of the simulation results.

3. Results and analysis

3.1. Changes in air pollutant concentration observed during the COVID-lock phase

The suspension of anthropogenic activities during the COVID-lock phase led to a significant reduction in the emissions of major pollutants over China. Wuhan was the first city to go into lockdown and had the strictest lockdown measures in China, which resulted in the most significant improvement in air quality (Zheng et al., 2020; Yao et al., 2021). There was a 22.8 μg m^{-3} (36.0%) decrease in Wuhan $PM_{2.5}$ concentrations during the COVID-lock phase compared to the pre-COVID phase, with main chemical components of $PM_{2.5}$ decreasing. As shown in Table 3, NO_3^- saw the largest decrease (56.1%), followed by NH_4^+ (46.4%), and EC (45.2%); these three components dominated the pollution decrease.

Surface wind speed was an important factor in determining the local accumulation, dispersion, and regional transport of pollutants. During the 2019 and pre-COVID phases, there was a high frequency of high $PM_{2.5}$ concentration events under quasi-static (0−1 m s^{-1}) and light (0−2 m s^{-1}) winds; however, the frequency was significantly lower at higher wind speeds (2−3, 3−4, and >4 m s^{-1}) (Fig. 3a). The $PM_{2.5}$ concentrations were higher at wind speeds of 3−4 m s^{-1} and significantly higher at wind speeds of >4 m s^{-1} (Fig. 3b). These results indicate that while local emissions were responsible for the majority of high $PM_{2.5}$ pollution events, $PM_{2.5}$ from long-distance pollution transport contributed significantly to the overall pollution levels. The relationship between $PM_{2.5}$ pollution and wind speed changed during the COVID-lock phase, with the frequency of high pollution events under quasi-static and light wind conditions decreasing remarkably compared to the pre-COVID and 2019 phases, but with a greater frequency under higher wind conditions (2−3 and 3−4 m s^{-1}) (Fig. 3a). The concentration of short-distance pollution transport under weak wind conditions (1−3 m s^{-1}) also increased compared to the pre-COVID and 2019 phases, while the concentration of long-range pollution transport with stronger wind (>4 m s^{-1}) decreased, especially compared to the 2019 phase (Fig. 3b). This indicates that, during the COVID-lock phase, reduced local emissions decreased the frequency of high $PM_{2.5}$ pollution events, and that cross-regional transport of air pollutants had a weaker effect on overall air pollution.

$PM_{2.5}$ concentrations in Wuhan were observed with a decrease by 36.0% during the COVID-lock phase compared to

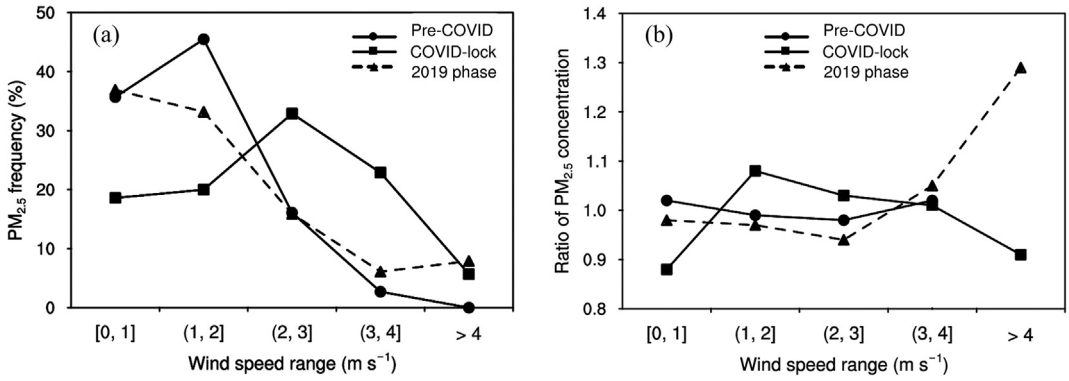

Fig. 3. Relationship between $PM_{2.5}$ concentration and 10-m wind speed intervals in Wuhan during the COVID-lock, pre-COVID, and 2019 phases (24 January–29 February 2019), (a) frequency of events where $PM_{2.5}$ concentrations exceeded 75 μg m^{-3} in the total pollution, (b) ratio of average $PM_{2.5}$ concentrations exceeded 75 μg m^{-3} to the total pollution.

the pre-COVID phase. In the following sections, we assessed how changes in meteorology, local emissions, and regional transport from external source emissions in the $PM_{2.5}$ source–receptor relationship contributed to the decrease in Wuhan's $PM_{2.5}$ concentration, by using FLEXPART-WRF and WRF-Chem modelling experiments.

3.2. Effect of meteorological changes and emissions reduction on $PM_{2.5}$ concentration

A series of $PM_{2.5}$ pollution control in recent years have resulted in a continuous improvement in air quality in China, even before the COVID-19 outbreak (Cai et al., 2017; Zheng et al., 2018; Zhang et al., 2019). As a result, a direct comparison of air pollution in 2020 with previous years may exaggerate the impact of COVID-19 on pollution reduction. Therefore, by comparing the changes in $PM_{2.5}$ concentration in the pre-COVID and COVID-lock phases, the impact of emissions reduction on $PM_{2.5}$ concentration in Wuhan during the COVID-19 period can be more reasonably understood.

First of all, considering the impact of meteorological changes on $PM_{2.5}$ concentration during the pre-COVID to COVID-lock phases, the air diffusion conditions from early January to late February were gradually improved from the perspective of seasonal transition. Tables 2 and 4 show that changes in meteorological conditions during the COVID-lock phase reduced $PM_{2.5}$ concentration in Wuhan by 8.0% compared with C1pre. The $PM_{2.5}$ level in the pre-COVID phase was then simulated using the adjusted COVID-lock emissions (C2pre), and compared with C1pre. This comparison showed that regional emissions reduction in China could reduce $PM_{2.5}$ concentration by 28.0%. The comparison of the simulation results of experiments C2 and C1pre show that changes in meteorological conditions and emissions reduction during the pre-COVID to COVID-lock phases jointly contributed to a 33.3% decrease in $PM_{2.5}$ concentration in Wuhan. This is very similar to the observed decrease of 36.0%. Therefore, compared with the pre-COVID phase, meteorological changes and emissions reduction during the COVID-lock phase decreased the $PM_{2.5}$ concentration in Wuhan by 22.2% and 77.8%, respectively (Tables 2 and 4).

In addition, there were significant differences in the emissions reduction effects under different meteorological conditions. The ventilation coefficient is a measure of the ground wind speed multiplied by the atmospheric boundary layer height. It was used to characterise the atmospheric dispersion capacity and its effect of the on the changes in local emissions reduction (experiment C3). The results of this experiment are shown in Fig. 4. The change in $PM_{2.5}$ concentration due to local emissions reduction has a logarithmic relationship with the ventilation coefficient. When the ventilation coefficient was less than the ~1500 m^2 s^{-1} threshold, the absolute value of the emissions reduction changes increased rapidly as the ventilation conditions became poor. The emissions reduction effect was the greatest when the diffusion conditions were extremely poor. When the ventilation coefficient exceeded the

Table 3
Changes in main $PM_{2.5}$ chemical components in Wuhan from the pre-COVID phase to the COVID-lock phase.

Component	Concentration Pre-COVID (μg m^{-3})	Concentration COVID-lock (μg m^{-3})	Percentage Change (%)
NO_3^-	29.85	13.11	–56.1
NH_4^+	17.12	9.17	–46.4
SO_4^{2-}	13.00	9.33	–28.2
OC	9.24	7.90	–14.5
TE	2.25	1.50	–33.3
EC	1.99	1.09	–45.2

Table 4
Impact and contribution of meteorological changes and regional emissions reduction in China on the decrease in $PM_{2.5}$ concentration in Wuhan from the pre-COVID to COVID-lock phase.

Description	Decrease in $PM_{2.5}$ concentration (%)
Meteorological changes	–8.0
Emissions reduction	–28.0
Meteorological changes and emissions reduction	–33.3
Contribution of meteorology changes	22.2
Contribution of emissions reduction	77.8

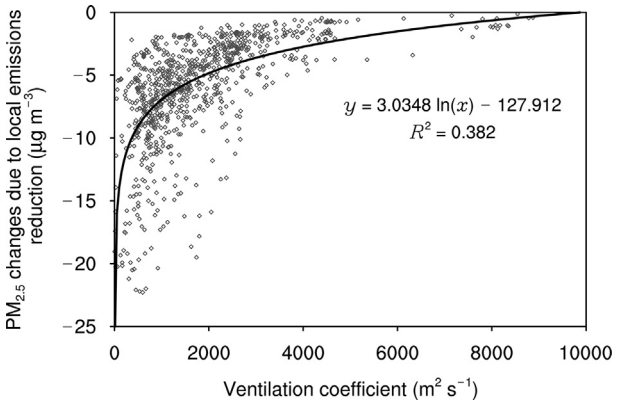

Fig. 4. Simulated hourly scattering relationship between the $PM_{2.5}$ changes due to local emissions reduction and ventilation coefficient during COVID-lock phase.

threshold, the atmospheric diffusion conditions were good, the emitted pollutants were diluted with atmospheric diffusion, and the effectiveness of emissions reduction was reduced. This suggests that the effectiveness of emissions reduction can be enhanced based on the daily variation pattern of the ventilation coefficient.

3.3. Effect of emissions reduction in Hubei and its surrounding areas from source−receptor relationship

The regional transport of air pollutants, controlled by emissions sources and meteorological factors, results in a complex source−receptor relationship of air pollution change (Yu et al., 2020). Fig. 5 shows the footprints of $PM_{2.5}$ in Wuhan during the different phases, to show the source−receptor relationship of air pollution changes. Overall, the potential sources of $PM_{2.5}$ in Wuhan were mainly concentrated in the eastern, northern, and north-eastern regions surrounding Hubei. External sources in the upstream regions contributed more to the $PM_{2.5}$ concentration in Wuhan as they were influenced by the winter monsoon, for example eastern Henan, south-eastern Shanxi, northern Jiangxi, and the majority of the Anhui province. The sources of $PM_{2.5}$ in Wuhan during the COVID-lock were mainly distributed across eastern Hubei and its upstream area, and were dominated by short-distance transport in the urban circle of Wuhan. The potential contribution of extra-provincial sources to the $PM_{2.5}$ in Wuhan during the pre-COVID, COVID-lock, and the 2019 phases were 40.0%, 20.0%, and 30.0%, respectively. This shows that the potential sources of $PM_{2.5}$ in the COVID-lock phase were more locally distributed.

The key emissions source areas (Hubei and its surrounding areas) (Fig. 1b) that impacted the $PM_{2.5}$ concentration in Wuhan during the COVID-lockdown were identified using the FLEXPART-WRF footprints. From Table 5, it can be seen that regional emissions reduction in China of 30% during the COVID-lock phase caused a reduction in $PM_{2.5}$ concentration in Wuhan by 27.5%, while the same emissions reduction in Hubei, the surrounding areas, and other regions caused a $PM_{2.5}$ concentration reduction in Wuhan by 13.7%, 10.9%, and 3.0%, respectively. Local and external emissions reduction decreased the $PM_{2.5}$ concentration in Wuhan equally. During the COVID-lock phase, Hubei, the surrounding areas, and other regions were responsible for 49.7%, 39.6%, and 10.7% of the reduction in $PM_{2.5}$ concentration in Wuhan, respectively. This revealed that regional-joint control measures in key areas accounted for 89.3% of the decrease in $PM_{2.5}$ concentration in Wuhan.

Table 5
Impact and contribution of different emissions reduction scenarios on the decrease in $PM_{2.5}$ concentration in Wuhan during the COVID-lock phase.

Description	Result (%)
Impact of 30% regional emissions reduction in China	−27.5
Impact of 30% emissions reduction in Hubei	−13.7
Impact of 30% emissions reduction in the surrounding areas	−10.9
Impact of 30% emissions reduction in other regions	−3.0
Contribution of emissions reduction in Hubei	49.7
Contribution of emissions reduction in the surrounding areas	39.6
Contribution of emissions reduction in other regions	10.7

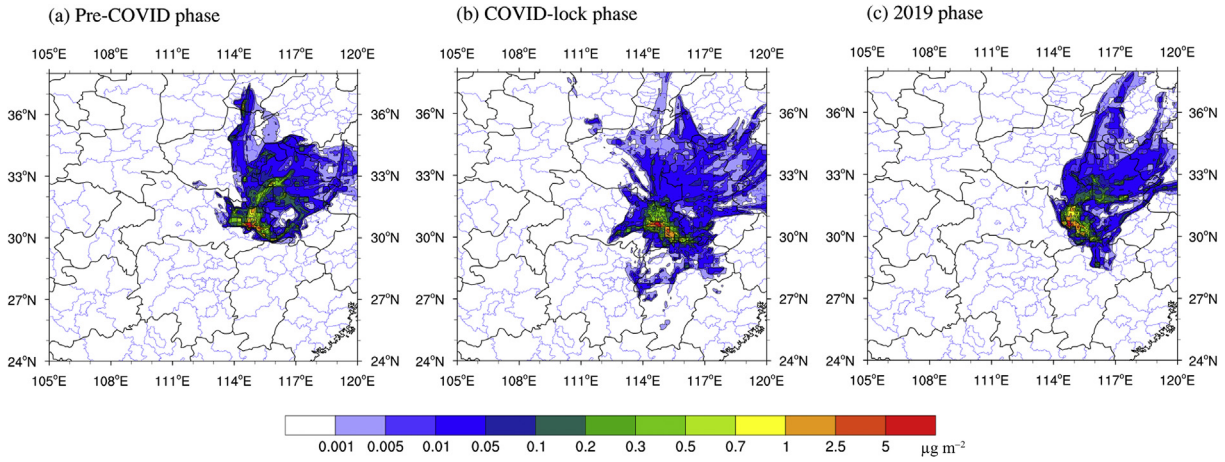

Fig. 5. Footprints of $PM_{2.5}$ in Wuhan from 48-h backward simulation using the FLEXPART model, (a) pre-COVID phase, (b) COVID-lock phase, (c) 2019 phase (24 January–29 February 2019).

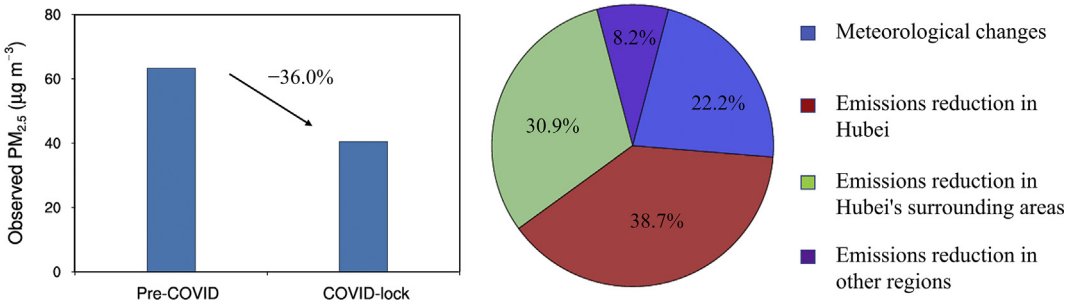

Fig. 6. Contribution of meteorology and emissions changes to the decrease in $PM_{2.5}$ concentration in Wuhan during pre-COVID and COVID-lock phases.

Fig. 6 summarises the contributions of different sources to the decrease in $PM_{2.5}$ concentration in Wuhan during the COVID-lock phase. Compared with the pre-COVID phase, the observed $PM_{2.5}$ concentration decreased by 22.8 μg m^{-3} (36.0%) during the COVID-lock phase. Of this decrease, 22.2% was due to changes in favourable meteorological conditions, and 77.8% was from regional emissions reduction in China, with Hubei, the surrounding areas and other regions contributing to 38.7%, 30.9% and 8.2% of the decrease in $PM_{2.5}$ concentration. Emissions reduction in local and external sources had a comparable effect on the decrease in $PM_{2.5}$ concentration in Wuhan, corresponding to 38.7% and 39.1% of the total reduction, respectively. Driven by atmospheric circulation, regional transport of air pollutants from upwind source regions can deteriorate the air quality in the downwind receptor regions. Therefore, the emissions reduction from the upwind source regions is an important contributor to the local decrease in $PM_{2.5}$ concentration in the downstream receptor.

In experiments C5 and C6, local emissions in Hubei and the Wuhan city circle were reduced by 50%. The results of these experiments showed that reducing the emissions in Hubei and the Wuhan city circle by 50% resulted in a 40.7 and 41.7 μg m^{-3} in $PM_{2.5}$ concentration in Wuhan, respectively. However, it was very similar to the reduction caused by the emissions reduction in the surrounding area by only 30% (40.9 μg m^{-3} $PM_{2.5}$). This shows that emissions reduction in the key areas along the pathway of regional transport can exert a large impact on improving air quality, as an efficient regional-joint control for decreasing $PM_{2.5}$ concentrations. Controlling key emissions source areas can greatly reduce the cost of emissions reduction.

4. Discussion and conclusions

In the COVID-lock period, it is shown that the local accumulation of air pollutants in Wuhan and cross-regional transport effects are weakened during low-emissions scenarios. The observed $PM_{2.5}$ concentration in Wuhan decreased by 22.8 μg m^{-3} (36.0%) from the pre-COVID to the COVID-lock phase, with 22.2% of that decrease resulting from the change in favourable meteorological conditions, and 77.8% resulting from regional emissions reduction in China. During the COVID-lock phase, emissions reduction in Hubei, the surrounding areas (Henan, Shandong, Anhui, Jiangsu and Jiangxi), and other regions were responsible for 49.7%, 39.6%, and 10.7% of the 77.8% reduction resulting from regional total emissions reduction in China, respectively. This shows that the significant decrease in $PM_{2.5}$ concentration in Wuhan is a positive effect of the passive implementation of regional-joint control in the surrounding provinces, with local emissions reduction in Hubei as the core. Therefore, we highlighted the importance of regional-joint control of air pollution, suggesting that emissions reduction in upwind source regions are an important contributor to the local decrease in $PM_{2.5}$ concentration in a downstream receptor.

This study identifying the source–receptor relationship of regional $PM_{2.5}$ transport in $PM_{2.5}$ reduction during the COVID-19 lockdown in Wuhan, China. Further research will be required on pollution effects, such as the impact of ozone pollution, air quality and human health, as well as the influence of greenhouse gas emissions reduction on climate change. Joint prevention and control is also one of the conventional methods to reduce the impact of climate change, such as controlling the increasing temperature to 1.5 °C through rapid emissions reduction. Possible uncertainties exist in this study due to the lack of real-time data of air pollutant emissions in the COVID-19 lockdowns. Using more up-to-date emissions data in chemical transport models in future studies could improve our understanding of the changes in pollutant concentrations during the COVID-19 lockdowns.

Declaration of competing interest

The authors declare no conflict of interests.

Acknowledgments

This research was supported by the special project “The impact of weather conditions on the spread of pandemic influenza virus (2020xtzx004)” from Collaborative Innovation Center on Forecast and Evaluation of Meteorological Disasters, Nanjing University of Information Science and Technology, and the National Natural Science Foundation of China (42075186; 41830965).

Appendix A. Supplementary data

Supplementary data to this article can be found online at https://doi.org/10.1016/j.accre.2021.09.013.

References

Bai, Y., Qi, H., Liu, L., et al., 2016. Development and preliminary application of environmental meteorology numerical model system in central China. Plateau. Meteor 35 (6), 1671−1682. https://doi.org/10.7522/j.issn.1000-0534.2015.00086 (Chinese.

Bai, Y., Qi, H., Zhao, T., et al., 2020. Simulation of the responses of rainstorm in the Yangtze River Middle Reaches to changes in anthropogenic aerosols emissions. Atmos. Environ. 220, 117081. https://doi.org/10.1016/j.atmosenv.2019.117081.

Bao, R., Zhang, A., 2020. Does lockdown reduce air pollution? Evidence from 44 cities in northern China. Sci. Total Environ. 731, 139052. https://doi.org/10.1016/j.scitotenv.2020.141419.

Cai, S., Wang, Y., Zhao, B., et al., 2017. The impact of the "air pollution prevention and control action plan" on $PM_{2.5}$ concentrations in Jing–Jin–Ji region during 2012−2020. Sci. Total Environ. 580, 197−209. https://doi.org/10.1016/j.scitotenv.2016.11.188.

Chang, X., Wang, S., Zhao, B., et al., 2019. Contributions of inter-city and regional transport to $PM_{2.5}$ concentrations in the Beijing-Tianjin-Hebei region and its implications on regional joint air pollution control. Sci. Total Environ. 660, 1191−1200. https://doi.org/10.1016/j.scitotenv.2018.12.474.

Chang, Y., Huang, R.J., Ge, X., et al., 2020. Puzzling haze events in China during the coronavirus (COVID-19) shutdown. Geophys. Res. Lett. 47, e2020GL088533. https://doi.org/10.1029/2020GL088533.

Chen, Y., Zhang, S., Peng, C., et al., 2020. Impact of the COVID-19 pandemic and control measures on air quality and aerosol light absorption in Southwestern China. Sci. Total Environ. 749, 141419. https://doi.org/10.1016/j.scitotenv.2020.141419.

Chen, Z., Xie, X., Cai, J., et al., 2018. Understanding meteorological influences on $PM_{2.5}$ concentrations across China: a temporal and spatial perspective. Atmos. Chem. Phys. 18, 5343−5358. https://doi.org/10.5194/acp-18-5343-2018.

Cheng, J., Su, J., Cui, T., et al., 2019. Dominant role of emission reduction in $PM_{2.5}$ air quality improvement in Beijing during 2013−2017: a model-based decomposition analysis. Atmos. Chem. Phys. 19, 6125−6146. https://doi.org/10.5194/acp-19-6125-2019.

Dai, Q., Liu, B., Bi, X., et al., 2020. Dispersion normalized PMF provides insights into the significant changes in source contributions to $PM_{2.5}$ after the COVID-19 outbreak. Environ. Sci. Technol. 54, 9917−9927. https://doi.org/10.1021/acs.est.0c02776.

El-Sayed, M.M.H., Elshorbany, Y.F., Koehler, K., 2021. On the impact of the COVID-19 pandemic on air quality in Florida. Environ. Pollut. 117451. https://doi.org/10.1016/j.envpol.2021.117451.

Fadnavis, S., Sabin, T.P., Rap, A., et al., 2021. The impact of COVID-19 lockdown measures on the Indian summer monsoon. Environ. Res. Lett. 16, 074054. https://doi.org/10.1088/1748-9326/ac109c.

Fan, C., Li, Y., Guang, J., et al., 2020. The impact of the control measures during the COVID-19 outbreak on air pollution in China. Rem. Sens. 12, 1613. https://doi.org/10.3390/rs12101613.

Forster, P.M., Forster, H.I., Evans, M.J., et al., 2020. Current and future global climate impacts resulting from COVID-19. Nat. Clim. Change 10, 913−919. https://doi.org/10.1038/s41558-020-0883-0.

Grell, G.A., Peckham, S.E., Schmitz, R., et al., 2005. Fully coupled "online" chemistry within the WRF model. Atmos. Environ. 39, 6957−6975. https://doi.org/10.1016/j.atmosenv.2005.04.027.

Grewe, V., Gangoli Rao, A., Grönstedt, T., et al., 2021. Evaluating the climate impact of aviation emission scenarios towards the Paris agreement including COVID-19 effects. Nat. Commun. 12, 3841. https://doi.org/10.1038/s41467-021-24091-y.

Griffith, S.M., Huang, W.S., Lin, C.C., et al., 2020. Long-range air pollution transport in East Asia during the first week of the COVID-19 lockdown in China. Sci. Total Environ. 741, 140214. https://doi.org/10.1016/j.scitotenv.2020.140214.

Hammer, M.S., van Donkelaar, A., Martin, R.V., et al., 2021. Effects of COVID-19 lockdowns on fine particulate matter concentrations. Sci. Adv. 7, eabg7670. https://doi.org/10.1126/sciadv.abg7670.

Huang, X., Ding, A., Gao, J., et al., 2020. Enhanced secondary pollution offset reduction of primary emissions during COVID-19 lockdown in China. Natl. Sci. Rev. nwaa137. https://doi.org/10.1093/nsr/nwaa137.

Jiang, Z., Shi, H., Zhao, B., et al., 2021. Modeling the impact of COVID-19 on air quality in southern California: implications for future control policies. Atmos. Chem. Phys. 21, 8693−8708. https://doi.org/10.5194/acp-21-8693-2021.

Kumar, R., Barth, M.C., Pfister, G.G., et al., 2014. WRF-Chem simulations of a typical pre-monsoon dust storm in northern India: influences on aerosols optical properties and radiation budget. Atmos. Chem. Phys. 14, 2431−2446. https://doi.org/10.5194/acp-14-2431-2014.

Kumar, S., Dwivedi, S.K., 2021. Impact on particulate matters in India's most polluted cities due to long-term restriction on anthropogenic activities. Environ. Res. 111754. https://doi.org/10.1016/j.envres.2021.111754, 2021.

Lennartson, E.M., Wang, J., Gu, J., et al., 2018. Diurnal variation of aerosols optical depth and $PM_{2.5}$ in South Korea: a synthesis from AERONET, satellite (GOCI), KORUS-AQ observation, and the WRF-Chem model. Atmos. Chem. Phys. 18, 15125−15144. https://doi.org/10.5194/acp-18-15125-2018.

Le, T., Wang, Y., Liu, L., et al., 2020. Unexpected air pollution with marked emission reductions during the COVID-19 outbreak in China. Science 369 (6504), 702−706. https://doi.org/10.1126/science.abb7431.

Li, L., Li, Q., Huang, L., et al., 2020. Air quality changes during the COVID-19 lockdown over the Yangtze River Delta region: an insight into the impact of human activity pattern changes on air pollution variation. Sci. Total Environ. 732, 139282. https://doi.org/10.1016/j.scitotenv.2020.139282.

Li, M., Zhang, Q., Kurokawa, J., et al., 2017. MIX: a mosaic Asian anthropogenic emission inventory under the international collaboration framework of the MICS-Asia and HTAP. Atmos. Chem. Phys. 17, 935−963. https://doi.org/10.5194/acp-17-935-2017.

Li, M., Yuan, K., Hu, K., et al., 2019. Trigger mechanism and main factors of urban heavy pollution processes in Wuhan. Torrential Rain Disaster 38 (6), 624−631. https://doi.org/10.3969/j.issn.1004-9045.2019.06.007 (Chinese).

Lian, X., Huang, J., Huang, R., et al., 2020. Impact of city lockdown on the air quality of COVID-19-hit of Wuhan city. Sci. Total Environ. 742, 140556. https://doi.org/10.1016/j.scitotenv.2020.140556.

Liu, F., Page, A., Strode, S.A., et al., 2020a. Abrupt decline in tropospheric nitrogen dioxide over China after the outbreak of COVID-19. Sci. Adv. 6 (28), eabc2992. https://doi.org/10.1126/sciadv.abc2992.

Liu, L., Bai, Y., Lin, C., et al., 2018. Evaluation of regional air quality numerical forecasting system in central China and its application for aerosols radiative effect. Meteorol. Mon. 44 (9), 1179−1190. https://doi.org/10.7519/j.issn.1000–0526.2018.09.006 (Chinese.

Liu, Q., Sha, D., Liu, W., et al., 2020b. Spatiotemporal patterns of COVID-19 impact on human activities and environment in mainland China using nighttime light and air quality data. Rem. Sens. 12, 1576. https://doi.org/10.3390/rs12101613.

Lu, M., Tang, X., Wang, Z., et al., 2017. Source tagging modeling study of heavy haze episodes under complex regional transport processes over Wuhan megacity, central China. Environ. Pollut. 231, 612−621. https://doi.org/10.1016/j.envpol.2017.08.046.

Mahato, S., Pal, S., Ghosh, K.G., 2020. Effect of lockdown amid COVID-19 pandemic on air quality of the megacity Delhi, India. Sci. Total Environ. 730, 139086. https://doi.org/10.1016/j.scitotenv.2020.139086.

Munir, S., Luo, Z., Dixon, T., 2021. Comparing different approaches for assessing the impact of COVID-19 lockdown on urban air quality in Reading, UK. Atmos. Res. 105730. https://doi.org/10.1016/j.atmosres.2021.105730, 2021.

Paolo, C., Jgor, A., Federico, S., et al., 2021. Negative ozone anomalies at a high mountain site in northern Italy during 2020: a possible role of COVID-19 lockdowns? Environ. Res. Lett. 16, 074029. https://doi.org/10.1088/1748-9326/ac0b6a.

Pei, Z., Han, G., Ma, X., et al., 2020. Response of major air pollutants to COVID-19 lockdowns in China. Sci. Total Environ. 743, 140879. https://doi.org/10.1016/j.scitotenv.2020.140879.

Rosenbloom, D., Markard, J., 2021. A COVID-19 recovery for climate. Science 368, 447. https://doi.org/10.1126/science.abc4887.

Shen, L., Zhao, T., Wang, H., et al., 2020. Importance of meteorology to air pollution events during the city lockdown for COVID-19 in Hubei Province, central China. Sci. Total Environ. 754, 142227. https://doi.org/10.1016/j.scitotenv.2020.142227.

Shi, X., Brasseur, G.P., 2020. The response in air quality to the reduction of Chinese economic activities during the COVID-19 outbreak. Geophys. Res. Lett. 47. https://doi.org/10.1029/2020GL088070 e2020GL088070.

Sun, Y., Lei, L., Zhou, W., et al., 2020. A chemical cocktail during the COVID-19 outbreak in Beijing, China: insights from six-year aerosol particle composition measurements during the Chinese New Year holiday. Sci. Total Environ. 742, 140739. https://doi.org/10.1016/j.scitotenv.2020.140739.

Tian, H., Liu, Y., Li, Y., et al., 2020. An investigation of transmission control measures during the first 50 days of the COVID-19 epidemic in China. Science 368 (6491), 638−642. https://doi.org/10.1126/science.abb6105.

Vega, E., Namdeo, A., Bramwell, L., et al., 2021. Changes in air quality in Mexico City, London and Delhi in response to various stages and levels of lockdowns and easing of restrictions during COVID-19 pandemic. Environ. Pollut. 117664. https://doi.org/10.1016/j.envpol.2021.117664.

Wang, P., Chen, K., Zhu, S., et al., 2020. Severe air pollution events not avoided by reduced anthropogenic activities during COVID-19 outbreak. Resour. Conserv. Recycl. 158, 104814. https://doi.org/10.1016/j.resconrec.2020.104814.

Xu, Y., Xue, W., Lei, Y., et al., 2018. Impact of meteorological conditions on $PM_{2.5}$ pollution in China during winter. Atmosphere 9, 429. https://doi.org/10.3390/atmos9110429.

Xue, W., Shi, X., Yan, G., et al., 2021. Impacts of meteorology and emission variations on the heavy air pollution episode in North China around the 2020 Spring Festival. Sci. China Earth Sci. 64 (2), 329−339. https://doi.org/10.1007/s11430-020-9683-8.

Yang, Q., Wang, B., Wang, Y., et al., 2021. Global air quality change during COVID-19: a synthetic analysis of satellite, reanalysis and ground station data. Environ. Res. Lett. 16, 074052.

Yao, L., Kong, S., Zheng, H., et al., 2021. Co-benefits of reducing $PM_{2.5}$ and improving visibility by COVID-19 lockdown in Wuhan. NPJ Clim. Atmos. Sci. 4, 40. https://doi.org/10.1038/s41612-021-00195-6.

Yin, Z., Zhang, Y., Wang, H., et al., 2021. Evident $PM_{2.5}$ drops in the east of China due to the COVID-19 quarantine measures in February. Atmos. Chem. Phys. 21, 1581−1592. https://doi.org/10.5194/acp-21-1581-2021.

Yu, C., Zhao, T., Bai, Y., et al., 2020. Heavy air pollution with a unique "non-stagnant" atmospheric boundary layer in the Yangtze River middle basin aggravated by regional transport of $PM_{2.5}$ over China. Atmos. Chem. Phys. 20, 7217−7230. https://doi.org/10.5194/acp-20-7217-2020.

Yuan, Qi, Qi, B., Hu, D., et al., 2020. Spatiotemporal variations and reduction of air pollutants during the COVID-19 pandemic in a megacity of Yangtze River Delta in China. Sci. Total Environ. 751, 141820. https://doi.org/10.1016/j.scitotenv.2020.141820.

Yue, Y., Wang, X., Zhang, M., et al., 2016. Air quality condition in Wuhan and its relationship to meteorological factors. Torrential Rain Disaster 35 (3), 271−278. https://doi.org/10.3969/j.issn.1004–9045.2016.03.010 (Chinese.

Zangari, S., Hill, D.T., Charette, A.T., et al., 2020. Air quality changes in New York City during the COVID-19 pandemic. Sci. Total Environ. 742, 140496. https://doi.org/10.1016/j.scitotenv.2020.140496.

Zhang, H., Wang, S., Hao, J., et al., 2016. Air pollution and control action in Beijing. J. Clean. Prod. 112, 1519−1527. https://doi.org/10.1016/j.jclepro.2015.04.092.

Zhang, W., Wang, H., Zhang, X., et al., 2020. Evaluating the contributions of changed meteorological conditions and emission to substantial reductions of $PM_{2.5}$ concentration from winter 2016 to 2017 in central and eastern China. Sci. Total Environ. 716, 136892. https://doi.org/10.1016/j.scitotenv.2020.136892.

Zhang, X., Xu, X., Ding, Y., et al., 2019. The impact of meteorological changes from 2013 to 2017 on $PM_{2.5}$ mass reduction in key regions in China. Sci. China Earth Sci. 62, 1885−1902. https://doi.org/10.1007/s11430-019-9343-3.

Zheng, B., Tong, D., Li, M., et al., 2018. Trends in China's anthropogenic emissions since 2010 as the consequence of clean air actions. Atmos. Chem. Phys. 18, 14095−14111. https://doi.org/10.5194/acp-18-14095-2018.

Zheng, B., Zhang, Q., Geng, G., et al., 2021. Changes in China's anthropogenic emissions and air quality during the COVID-19 pandemic in 2020. Earth Syst. Sci. Data 13, 2895−2907. https://doi.org/10.5194/essd-13-2895-2021.

Zheng, H., Kong, S., Wu, F., et al., 2019. Intra-regional transport of black carbon between the south edge of the North China Plain and central China during winter haze episodes. Atmos. Chem. Phys. 19, 4499−4516. https://doi.org/10.5194/acp-19-4499-2019.

Zheng, H., Kong, S., Chen, N., et al., 2020. Significant changes in the chemical compositions and sources of $PM_{2.5}$ in Wuhan since the city lockdown as COVID-19. Sci. Total Environ. 739, 140000. https://doi.org/10.1016/j.scitotenv.2020.140000.

Zhong, M., Saikawa, E., Liu, Y., et al., 2016. Air quality modeling with WRF-Chem v3.5 in East Asia: sensitivity to emissions and evaluation of simulated air quality. Geosci. Model Dev. (GMD) 9, 1201−1218. https://doi.org/10.5194/gmd-9-1201-2016.

Zhou, W., Gao, M., He, Y., et al., 2019. Response of aerosols chemistry to clean air action in Beijing, China: insights from two-year ACSM measurements and model simulations. Environ. Pollut. 255, 113345. https://doi.org/10.1016/j.envpol.2019.113345.